

Mössbauer Effect in $\text{Te}^{125}\dagger$

CHARLES E. VIOLET AND REX BOOTH

Lawrence Radiation Laboratory, University of California, Livermore, California

(Received 1 November 1965)

The Mössbauer effect associated with the 35.6-keV transition of Te^{125} has been investigated in the host materials ZnTe, MnTe, βFeTe , Te, TeO_2 , Na_2TeO_3 , TeF_4 , TeI_4 , Cu, and NaIO_3 . Quadrupole splitting is not observed in host materials of cubic symmetry, i.e., ZnTe and Cu. The host materials of noncubic symmetry all exhibit quadrupole splitting. The quadrupole splitting in Te at 4.8°K is $(0.90 \pm 0.03) \times 10^{-6}$ eV (0.76 ± 0.02 cm/sec). The temperature dependence of the quadrupole splitting in Te between 4.8 and 77.9°K implies a molecular torsional frequency of $\approx 6 \times 10^{12}$ sec⁻¹. I^{125} incorporated into a Cu matrix as a Mössbauer source gives a single resonance line, while I^{125} in a NaIO_3 source gives four resonance lines. The latter spectrum is interpreted on the hypothesis that Te^{125} is produced in two observable charge states following the decay of I^{125} in NaIO_3 . The two charge states may result from *K* x-ray and Auger transitions following the I^{125} decay. In this model the higher charge state decays by electron capture with a half-life of $\approx 1.6 \times 10^{-9}$ sec. The recoilless fraction for the Cu source at 82°K is ≈ 0.2 . In NaIO_3 it is 0.14 (82°K) and 0.28 (4.8°K). This corresponds to an apparent NaIO_3 Debye temperature of $\approx 155^\circ\text{K}$.

I. INTRODUCTION

BY using the Mössbauer effect associated with the 35.6-keV transition from the first excited state to the ground state in Te^{125} , we have obtained new information on the Te^{125} nucleus and the properties of pure Te and Te compounds. A determination of the electric quadrupole moment of the Te^{125} 35.6-keV level, $[|Q| = (0.20_{-0.02}^{+0.03}) \times 10^{-24}$ cm²]¹ and a description of the Mössbauer spectrometer, the I^{129} source spectrum, and the detecting system have been previously published.² We have been primarily interested in (1) measuring quadrupole splitting, isomer shift, and in some cases the magnitude of the resonance absorption; and (2) inferring nuclear and solid state physics information from these data. During the course of this work, other investigations of Te^{125} have been reported.³⁻⁹ Included in our analysis is a comparison of some of this information with our results.

II. CRYOSTATS, SOURCES, AND ABSORBERS

Two types of cryostats were used to cool the sources and absorbers. Small, movable, liquid nitrogen (LN) cryostats² were used to maintain source or absorber temperatures at $(82 \pm 1)^\circ\text{K}$. A large, stationary cryostat

maintained samples at 4.8, 20.9, 63.8, and 77.9°K, using liquid He, H₂, N₂ (pumping), and N₂ (atmospheric pressure), respectively. Sample temperatures in the stationary cryostat were measured by a calibrated carbon resistor and in the LN cryostats by a thermocouple.

The source of resonance radiation was I^{125} (60 day half-life) which decays by electron capture directly to the 35.6-keV ¹⁰ level of Te^{125} .¹¹ The transition to the ground state is *M1* with less than 1% electric quadrupole admixture, and the fraction of unconverted gammas is 0.07 ± 0.02 .¹² The excited state half-life is $(1.58 \pm 0.15) \times 10^{-9}$ sec.¹³

Resonance emission spectra of I^{125} in four host materials—Cu, NaIO_3 , NaI, and I₂—were measured. That the emission spectra for the Cu source was a single line was verified using a ZnTe absorber (Fig. 1). For the NaIO_3 source it consisted of several unresolved lines. These two sources gave a readily observed effect, and both were used in this experiment. The resonance emission spectra from the NaI and I₂ sources were similar to the NaIO_3 source, but the effect was too small for them to be of use. The Cu source was prepared¹⁴ by the electro-deposition of 60 mCi of I^{125} on a Cu foil, coating this surface with a thin layer of Cu, and then annealing. The NaIO_3 source was prepared from polycrystalline NaIO_3 enriched with 40 mCi of I^{125} .¹⁵ This material was then embedded in a Lucite holder as a thin disk 1.27 cm in diameter and 39.5 mg/cm² thick.

The Te absorbers were prepared from samples of various enrichments of Te^{125} ($40\% \leq \text{Te}^{125}/\text{Te} \leq 78\%$).¹⁵ The ZnTe, MnTe, βFeTe , TeF_4 , TeI_4 , TeO_2 , and

[†] Work performed under the auspices of the U. S. Atomic Energy Commission.

¹ C. E. Violet, Rex Booth, and F. Wooten, *Phys. Letters* **5**, 230 (1963).

² R. Booth and C. E. Violet, *Nucl. Instr. Methods* **25**, 1 (1963).

³ Phan Zuy Hein, V. G. Shapiro, and V. S. Spinel, *Zh. Eksperim. i Teor. Fiz.* **42**, 703 (1962) [English transl.: *Soviet Phys.—JETP* **15**, 489 (1962)].

⁴ N. Shikazono, T. Shoji, H. Takekoshi, and P. K. Tseng, *J. Phys. Soc. Japan* **17**, 1205 (1962).

⁵ R. B. Frankel, P. H. Barrett, and D. A. Shirley, *Bull. Am. Phys. Soc.* **7**, 600 (1962).

⁶ Audrey B. Buyrn and L. Grodzins, *Bull. Am. Phys. Soc.* **8**, 43 (1963).

⁷ Naomoto Shikazono, *J. Phys. Soc. Japan* **18**, 925 (1963).

⁸ E. P. Stepanov, K. P. Aleshin, R. A. Manapov, B. N. Samoilov, V. V. Sklyarevsky, and V. G. Stankevich, *Phys. Letters* **6**, 155 (1963).

⁹ J. J. Huntzicker, R. B. Frankel, N. J. Stone, and D. A. Shirley, *Bull. Am. Phys. Soc.* **9**, 741 (1964).

¹⁰ R. S. Narcisi, Technical Report No. 2-9, Department of Physics, Harvard University, Cambridge, Massachusetts (unpublished).

¹¹ *Nuclear Data Sheets*, compiled by K. Way *et al.* (Printing and Publishing Office, National Academy of Sciences—National Research Council, Washington, 25, D. C., 1958).

¹² J. C. Bowe and P. Axel, *Phys. Rev.* **85**, 858 (1952).

¹³ R. L. Graham and R. E. Bell, *Can. J. Phys.* **31**, 377 (1953).

¹⁴ Obtained from Nuclear Science and Engineering Corporation, Pittsburgh, Pennsylvania.

¹⁵ Obtained from Oak Ridge National Laboratory, Oak Ridge, Tennessee.

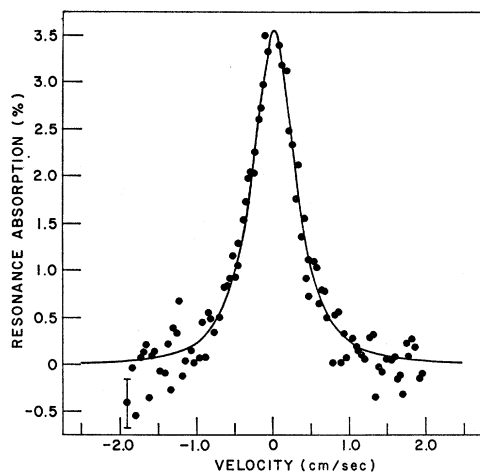


FIG. 1. Resonance absorption spectrum from the Cu source at 82°K and the ZnTe absorber at 82°K.

Na_2TeO_3 absorbers contained the normal abundance of Te^{125} (7%). Absorbers were made by mixing uniformly the specified amount of material with a powdered thermoplastic. The mixture was then moulded under moderate heat and pressure into a thin disk 2.54 cm in diameter. X-ray diffraction patterns were obtained for all absorber materials by the Debye-Scherrer method. The TeO_2 was predominantly tetragonal ($\alpha\text{-TeO}_2$) with a small fraction in the orthorhombic phase. The diffraction lines from Na_2TeO_3 , TeF_4 , and TeI_4 showed that these materials were of noncubic symmetry and were nonstoichiometric. All other materials gave the expected pattern. Information on the absorbers used in this experiment is given in Table I.

III. SINGLE LINE SOURCE DATA

A spectrum obtained from a Te absorber is shown in Fig. 2. Spectra obtained from TeO_2 and Na_2TeO_3 absorbers are shown in Fig. 3. These spectra were analyzed by the method of least squares, using an IBM 7094 computer.

The resonance absorption (A) from a single line source and a double line absorber can be described

TABLE I. Absorber properties.

Absorber	Total thickness (mg/cm ²)	$\text{Te}^{125}/\text{Te}$ (%)	Te^{125} thickness (mg/cm ²)	$n\sigma_0$
ZnTe	44.2	7.0	2.0	...
MnTe	31.1	7.0	1.5	...
βFeTe	21.2	7.0	1.0	...
Te-1	4.3	78.8	3.4	4.2
Te-2	30.0	40.4	12.1	15.2
Te-3	30.3	71.0	21.5	27.0
TeO_2	46.0	7.0	2.6	...
Na_2TeO_3	52.4	7.0	2.1	...
TeF_4	48.9	7.0	1.7	...
TeI_4	71.0	7.0	1.0	...

TABLE II. Analysis of single line source data.

Absorber	Absorber temperature (°K)	$\frac{t}{2}$	$A_m(t/2)^a$ (%)	ϵ_a (cm/sec) ^b	δ (cm/sec) ^d	$A^{a,e}$ (% cm/sec)
ZnTe	82	...	2.0	<0.07	+0.008(7)	...
MnTe	82	0.16(7) ^c	+0.02(7)	...
βFeTe	82	0.15(7)	+0.05(7)	...
Te-1	4.8	1.0	5.3	0.374(5)	+0.044(7)	9.4
Te-2	4.8	3.6	13.5	0.384(3)	+0.051(4)	26
	20.9	3.2	12.6	0.381(3)	+0.053(3)	24
	63.8	1.5	9.9	0.379(2)	+0.049(2)	19
	77.9	1.1	8.1	0.368(6)	+0.053(7)	15
Te-3	82	1.8	7.9	0.388(9)	+0.069(9)	19
TeO_2	82	...	3.2	0.363(6)	+0.078(8)	...
Na_2TeO_3	82	...	2.1	0.33(1)	+0.04(1)	...
TeF_4	82	0.34(9)	+0.04(9)	...
TeI_4	82	0.30(9)	+0.10(9)	...

^a Corrected for background.

^b A Doppler shift of 1 cm/sec is equivalent to 1.19×10^{-6} eV or 288 Mc/sec.

^c The rms errors in the parameters are shown in parentheses as uncertainties in the final figure.

^d The center shifts are relative to the Cu source at 82°K.

^e Area under resonance spectrum obtained by numerical integration.

by¹:

$$A = A_m \left(\frac{t}{2} \right) \left\{ \left[1 + \left(\frac{2(\delta - v - \epsilon_a)}{\Gamma_1(t/2)} \right)^2 + \frac{1}{2} \left(\frac{2(\delta - v - \epsilon_a)}{\Gamma_2(t/2)} \right)^4 \right]^{-1} + \left[1 + \left(\frac{2(\delta - v + \epsilon_a)}{\Gamma_1(t/2)} \right)^2 + \frac{1}{2} \left(\frac{2(\delta - v + \epsilon_a)}{\Gamma_2(t/2)} \right)^4 \right]^{-1} \right\}, \quad (1)$$

where for a single source and absorber line

$A_m(t/2)$ = maximum resonance absorption,

δ = isomer shift,

$2\epsilon_a$ = quadrupole splitting in the absorber,

v = relative velocity (positive for decreasing source-absorber distance),

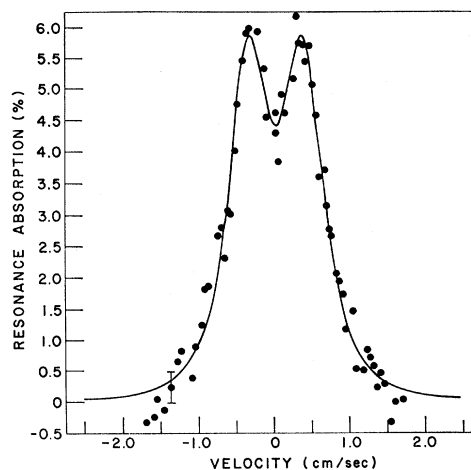


FIG. 2. Resonance absorption spectra from the Cu source at 82°K and Te-1 at 4.8°K.

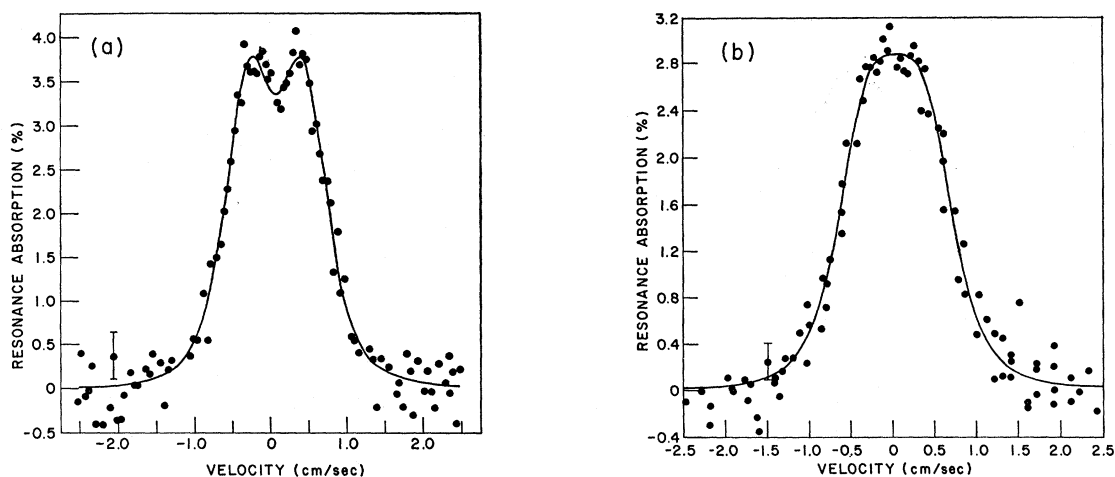


FIG. 3. Resonance absorption spectra from the Cu source at 82°K, and the (a) TeO₂ and (b) Na₂TeO₃ absorbers at 82°K.

$\Gamma_{1,2}(t/2)$ = line width parameters,

$$t = n\sigma_0 f_a,$$

n = number of Te¹²⁵ atoms/cm²,

σ_0 = maximum resonance cross section,

f_a = recoilless fraction for the absorber.

The best values of the parameters A_m , ϵ_a , δ are given with their rms errors in Table II. Using these values, Eq. (1) is compared with the corresponding spectra in Figs. 1, 2, and 3.

Values of the isomer shift and quadrupole splitting for MnTe, β FeTe, TeF₄, and TeI₄ absorbers were obtained by a graphical analysis. These and the associated rms errors are also given in Table II. The spectra for the MnTe and TeF₄ absorbers are shown in Figs 4 and 5, respectively. The spectrum from β FeTe is similar to

that of MnTe, and the spectrum from TeI₄ is similar to that of TeF₄.

A. Isomer Shifts and Quadrupole Splitting

1. Isomer Shifts

Values of the isomer shift for Te and Te compounds at liquid-helium and liquid-nitrogen temperatures are given in Table III. The results of other workers⁵⁻⁸ are also included in Table III. (The effect of the second-order Doppler shift can be neglected.) Buyrn and Grodzins⁶ have pointed out that the electron density at the Te nucleus in Na₂TeO₄ is less than in Te. This, combined with their measured isomer shift in Na₂TeO₄, led to the conclusion that the charge radius is larger in the excited state than in the ground state. Using this information and the measured quadrupole moment of

TABLE III. Isomer shifts^a and quadrupole splittings. (Quadrupole splittings are in italics.)

	Liquid-nitrogen temp.			Liquid-helium temp.		
	This work	Shikazono ^b	Stepanov, <i>et al.</i> ^c	This work	Frankel, <i>et al.</i> ^d	Buyrn and Grodzins ^e
ZnTe	-0.04(1) ^f	<0.07				
MnTe	-0.03(2)	0.3(1)	0			
β FeTe	0.00(2)	0.3(1)				
NiTe						-0.10(1) 0
PbTe			-0.09	0		
Te	0 ^a	0.74(2) ^g	0 0.7	0	0.77	0 0.75
Te (amorphous)			-0.04	0.66		
TeO ₂	+0.03(1)	0.73(1)	0.7	-0.03	{0.55 ^h 1.01}	0.57 0.70
Na ₂ TeO ₃	-0.01(1)	0.66(2)				
Na ₂ TeO ₄						-0.15(1) 0
Te in Cu	-0.05(1)	<0.07		-0.05(1)		
TeF ₄	-0.01(5)	0.7(1)				
TeI ₄	+0.05(5)	0.6(1)				

^a Isomer shifts are relative to a Te source at LN temperature or below.

^b Reference 7.

^c Reference 8.

^d Reference 5.

^e Reference 6.

^f The rms errors are shown in parentheses as uncertainties in the final figure.

^g Weighted mean.

^h Two pairs of lines.

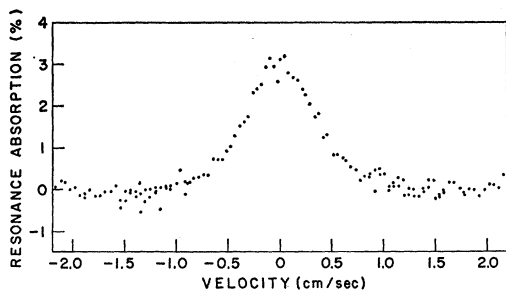


FIG. 4. Resonance absorption spectrum from the Cu source at 82°K and the MnTe absorber at 82°K.

the Te^{125} first excited state,^{1,7} an estimate of the charge radius difference has been given by Shirley¹⁶;

$$(\langle R_{\text{ex}}^2 \rangle - \langle R_{\text{gr}}^2 \rangle)^{1/2} / R \approx +9 \times 10^{-4}.$$

Te^{125} has 52 protons and 73 neutrons. The odd neutron, based on the single-particle model, occupies an $s_{1/2}$ state (ground level) or a $d_{3/2}$ state (first excited level). To a first approximation, neutron excitation would leave the charge radius unchanged. The fact that the charge radius does change is additional evidence that these states are mixed configurations rather than single-particle states.¹⁰

2. Quadrupole Splitting

Measurements of the Te^{125} quadrupole splitting in various materials, as determined by our measurements and those of other workers,⁵⁻⁸ are listed in Table III. With respect to this information we make the following observations:

(a) Quadrupole splitting is not observed, as expected, in fcc ZnTe, Cu, and PbTe; also it is not observed in hexagonal NiTe which is unexpected.

(b) In this work quadrupole splitting is observed in hexagonal MnTe at LN temperature, whereas Shikazono⁷ reports no quadrupole splitting in MnTe at this temperature. He considers MnTe to be a pure ionic crystal and concludes that the contribution to the electric field gradient from charges on neighboring ions is negligibly small. However, our MnTe data suggest that this conclusion is untenable. Also, calculations of

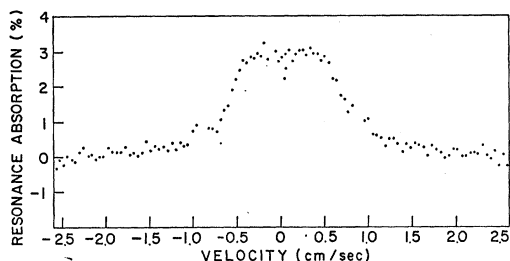


FIG. 5. Resonance absorption spectrum from the Cu source at 82°K and the TeF_4 absorber at 82°K.

¹⁶ D. A. Shirley, *Rev. Mod. Phys.* **36**, 339 (1964).

charge distributions in Te intermetallic compounds suggest that MnTe may not be, even approximately, an ionic crystal.¹⁷

(c) The weighted mean value of the quadrupole splitting in Te at 4.8°K is 0.76 ± 0.02 cm/sec which is equivalent to $(0.90 \pm 0.03) \times 10^{-6}$ eV or 219 ± 6 Mc.

B. The Temperature Dependence of the Quadrupole Splitting in Te

To interpret the temperature dependence of the quadrupole splitting between 4.8–77.9°K, we make the following assumptions: (1) the effect of any variation of the bonding character is negligible, and (2) the observed decrease in the quadrupole splitting with increasing temperature is the result of molecular torsional motions. The crystal structure¹⁸ of Te is depicted in Fig. 6(a). The atoms are arranged in spiral chains. The covalent bonding between atoms on the same chain is strong relative to the van der Waals bonding between chains. Therefore to a first approximation the chains can be treated as noninteracting molecules.¹

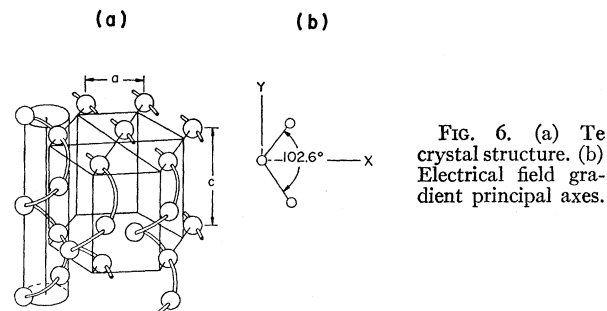


FIG. 6. (a) Te crystal structure. (b) Electrical field gradient principal axes.

The quadrupole splitting for spin $\frac{3}{2}$ in an axially symmetric field gradient is¹⁹

$$2\epsilon = \frac{1}{2} e^2 q Q (1 + \frac{1}{3} \eta^2)^{1/2}, \quad (2)$$

where

e = charge of the electron,

eq = the component of the electric field gradient (EFG) along the Z principal axis,

Q = electric quadrupole moment,

η = asymmetry parameter.

For oscillating atoms the splitting is also given by Eq. (2) in which (eq) and (η) are modified to describe the average EFG tensor.¹⁹ The modified parameters can be simplified using the following approximations: (1) the effect of the asymmetry parameter is negligible, and (2) the orientation of a Te atom relative to the EFG principal axes [Fig. 6(b)] is such that $A_{zx} \omega_x = A_{yz} \omega_y$, where

¹⁷ C. A. Coulson, L. B. Redei, and D. Stocker, *Proc. Roy. Soc. (London)* **A270**, 357 (1962).

¹⁸ R. W. G. Wyckoff, *Crystal Structures* (Interscience Publishers, Inc., New York, 1963), 2nd ed.

¹⁹ T. P. Das and E. L. Hahn, *Nuclear Quadrupole Resonance Spectroscopy* (Academic Press Inc., New York, 1958).

$A_{x,y}$ and $\omega_{x,y}$ are the moments of inertia and torsional frequencies, respectively, about the x,y principal axes.

In this approximation the temperature dependence of the quadrupole splitting is

$$2\epsilon(T) = 2\epsilon(0) \left[1 - \frac{3\hbar}{A\omega_c} (\exp(T_c/T) - 1)^{-1} \right], \quad (3)$$

where

$$A_x\omega_x = A_y\omega_y = A\omega_c, \\ \hbar T_c = \hbar\omega_c.$$

T_c is a characteristic temperature associated with a torsional frequency ω_c . Least-squares fitting of Eq. (3) to the data of Te-2 (Table II) yields

$$2\epsilon(0) = 0.766 \text{ cm/sec}, \\ 3\hbar/A\omega_c = 0.016, \\ T_c = 48^\circ\text{K}.$$

Equation (3) is plotted for these parameters and compared to the experimental data in Fig. 7.

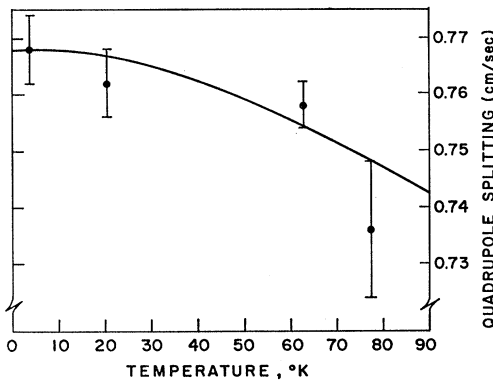


FIG. 7. Temperature dependence of the quadrupole splitting for Te-2.

The torsional frequency $\omega_c = 6.3 \times 10^{12} \text{ sec}^{-1}$ corresponds to a wave number of 33 (cm^{-1}). It would be of interest to check this value using optical methods. The optical transmission of Te has apparently not been measured for wave numbers less than $\approx 67 \text{ (cm}^{-1}\text{)}$.²⁰

IV. NaIO_3 SOURCE DATA

Resonance absorption spectra obtained from the NaIO_3 source have been analyzed by assuming an emission spectrum of four equal intensity lines. This is the simplest source spectrum that can account for the observed spectra. We postulate that the four emission lines are associated with two charge states of Te^{125} at iodine sites in NaIO_3 . Each charge state is associated with an emission line pair, and is characterized by an isomer shift and a quadrupole splitting.

²⁰ R. S. Caldwell and H. Y. Fan, Phys. Rev. **114**, 664 (1959).

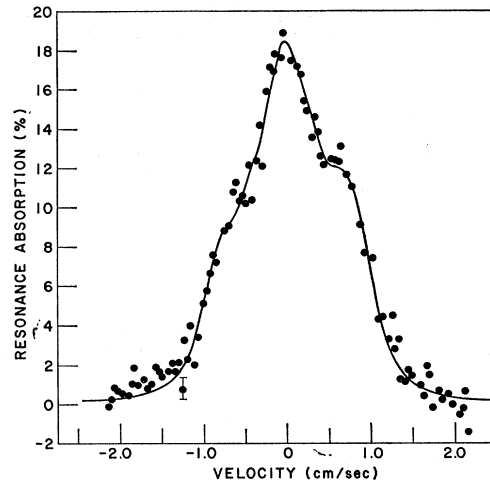


FIG. 8. Resonance absorption spectra from Te-2 at 82°K and the NaIO_3 source at 4.8°K .

Resonance absorption spectra obtained with this source and Te absorbers have been analyzed using an equation consisting of a sum of four terms each of the form of Eq. (1). This equation has been fitted to these data by least-squares analysis on an IBM 7094. The quadrupole splitting in $\text{Te}(2\epsilon_a)$ was assigned from Table II. It was possible to obtain simultaneously converging values of the parameters only for spectra in which the structure was not obscured by broadening due to absorber thickness. One of the spectra that met this condition is shown in Fig. 8. An analysis of these spectra yields (1) emission line energies, and (2) the recoilless fraction for the NaIO_3 source at 4.8 and 82°K .

A. Emission Line Energies

For the various spectra the energies of corresponding emission lines are in agreement within experimental error. Therefore, these have been combined and the weighted average line energies in units of the Doppler shift are given in Table IV. Four emission lines can be

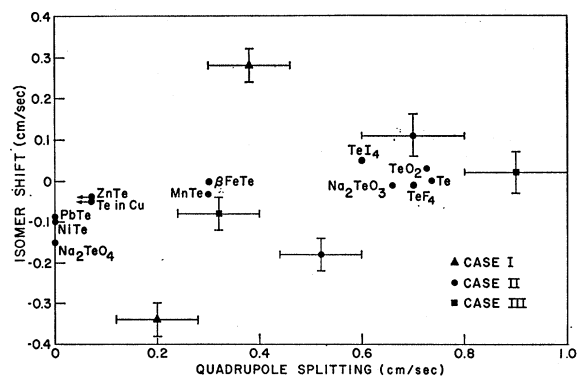


FIG. 9. The correlation of isomer shift with quadrupole splitting for Te and Te compounds. Values for the three cases of NaIO_3 source line groupings are also plotted.

TABLE IV. NaIO₃ source emission spectrum (82°K).
Weighted average emission line positions.^a

Line	Position (cm/sec)
1	-0.44(6)
2	-0.24(6)
3	+0.08(4)
4	+0.47(7)

^a The line positions are relative to the transition energy in Te.

grouped into two pairs of emission lines in three ways. The isomer shifts and quadrupole splittings for these three cases are specified in Table V.

To determine which of these cases could correspond to physical reality, we compare this information with the measured isomer shifts and quadrupole splittings of Te¹²⁵ in various chemical compounds. A plot of the information from Table III (Fig. 9) strongly suggests a correlation between the isomer shift and the quadrupole splitting.²¹ The values for three source-line groupings are also plotted in Fig. 9. Assuming that this correlation exists, the best agreement is obtained with Case III; Case I should be rejected and Case II is marginal. We conclude that the production of Te¹²⁵ in two observable charge states is a tenable explanation for the emission spectrum of resonance gammas from the NaIO₃ source.

Two charge states could be produced by *K* x ray and Auger transitions in the following way. Let us characterize the charge state resulting from the complete de-excitation of the atom by one *K* x ray as Te⁵⁺. Other *K*α and *K*β x rays are followed predominantly by Auger processes from the *L*, *M*, and *N* shells, resulting in a charge state characterized by Te⁶⁺.

Assuming that only these two charge states are produced, the initial frequency of the Te⁵⁺ state is

$$\frac{\text{Te}^{+5}}{\text{Te}^{+5} + \text{Te}^{+6}} = \left[1 + \left(\frac{L}{K} \right) \right]^{-1} [\omega_K] \left[\frac{N(K\beta \text{ max})}{N(K\alpha) + N(K\beta)} \right],$$

where $(L/K) = (L/K)$ capture ratio in the I¹²⁵ decay, $\omega_K = K$ shell fluorescent yield of Te, $N(K\beta \text{ max})/N(K\alpha) + N(K\beta) =$ fraction of complete *K* x ray de-excitations to total number of *K* x rays. This fraction is not known explicitly. However, an upper limit can

TABLE V. NaIO₃ source emission spectrum (82°K). Possible assignments of emission line pairs to two charge states.

Case	Lines	Δ^a (cm/sec)	ϵ (cm/sec)	Lines	Δ^a (cm/sec)	ϵ (cm/sec)
I	1 & 2	-0.34	0.10	3 & 4	+0.28	0.19
II	1 & 3	-0.18	0.26	2 & 4	+0.11	0.35
III	1 & 4	+0.02	0.45	2 & 3	-0.08	0.16

^a The isomer shifts of emission line pairs are relative to a Te source at LN temperature or below.

²¹ For a similar analysis of isomer shift and quadrupole splitting for the Fe⁵⁷ transition, see P. H. Remy and H. Pollak, J. Appl. Phys. 36, 860 (1965).

be obtained from the known intensity of the Te*K*β₂' x rays. Using the values¹¹

$$(L/K) = 0.25,$$

$$\omega_K = 0.86,$$

$$N(K\beta_2')/N(K\alpha + K\beta) = 0.030,$$

the initial frequency ratio of the lower to higher charge states is

$$R = \text{Te}^{+5}/\text{Te}^{+6} < 0.02. \quad (4)$$

However, in our analysis the four source lines have been shown to have nearly equal intensity. Therefore, the observed ratio is essentially

$$R_{\text{obs}} = 1. \quad (5)$$

One can account for this discrepancy by assuming that the higher charge state decays to the lower charge state by electron capture. Using this model the half-life (*T*_c) for the higher charge state is related to the half-life (*T*_{ex}) of the excited state by

$$T_c = T_{\text{ex}} \frac{R+1}{R_{\text{obs}} - R}. \quad (6)$$

(By definition $R_{\text{obs}} \geq R$.) Combining Eqs. (4), (5), and (6) we have

$$T_c \approx T_{\text{ex}} (= 1.6 \times 10^{-9} \text{ sec}).$$

The only Mössbauer isotope which has been extensively investigated in two or more charge states is Fe⁵⁷.²² In this case the life time of an observable charge state must be greater than $\approx 10^{-8}$ sec.

B. Recoilless Fraction of the NaIO₃ Source

The measured area under the resonance spectra yields the recoilless fraction of the NaIO₃ source at 4.8 and 82°K:

$$f_s(4.8^\circ\text{K}) = 0.14,$$

$$f_s(82^\circ\text{K}) = 0.28.$$

On the Debye model these values would correspond to a Debye temperature of $\theta \approx 155^\circ\text{K}$ for NaIO₃.

V. CONCLUSIONS

Quadrupole splitting is not observed in the host materials of cubic symmetry, i.e., ZnTe and Cu. In the remaining host materials, all of which have noncubic symmetry, quadrupole splitting is observed. The quadrupole splitting in Te at 4.8°K is $(0.90 \pm 0.03) \times 10^{-6}$ eV, which is equivalent to 0.76 ± 0.02 cm/sec or 219 ± 6 Mc.

The temperature dependence of the quadrupole splitting in Te between 4.8 and 77.9°K implies a molecular torsional frequency of $\approx 6 \times 10^{12}$ sec⁻¹ which

²² See, e.g., G. K. Werthein, *Mössbauer Effect* (Academic Press Inc., New York, 1964).

corresponds to a wave number of ≈ 33 (cm^{-1}). It would be of interest to check this value by optical techniques.

I^{125} incorporated into a Cu matrix as a Mössbauer source emits a single line of resonance gammas. I^{125} in a NaIO_3 source emits four lines of resonance gammas, all of nearly equal intensity. This implies that Te^{125} is produced in two observable charge states following the decay of I^{125} in NaIO_3 . The two charge states may result from the K x ray and Auger transitions following the I^{125} decay. In this model, the higher charge state decays to the lower charge state by electron capture with a half-life of $\approx 1.6 \times 10^{-9}$ sec.

The recoilless fraction of the Cu source at 82°K is ≈ 0.2 . In NaIO_3 it is 0.14 (82°K) and 0.28 (4.8°K).

This corresponds to a NaIO_3 Debye temperature of $\approx 155^\circ\text{K}$.

ACKNOWLEDGMENTS

We wish to thank V. G. Silveira for carrying out the x-ray diffraction measurements and R. E. Duncan for programming the least-squares fitting routines on the IBM 7094. The assistance of D. L. Davis in the early experimental work is gratefully acknowledged. Conversations with D. A. Shirley, F. Wooten, and D. N. Pippkorn have been valuable in the interpretation of our experimental results. We greatly appreciate the advice and encouragement of H. Mark and E. Goldberg.

Linear Relationship for Heavy-Ion Pulse Heights in Alkali Halides*

E. A. WOMACK, A. J. LAZARUS, AND S. W. W. LIU

Department of Physics and Laboratory for Nuclear Science, Massachusetts Institute of Technology, Cambridge, Massachusetts

(Received 19 October 1965)

It has been found that the total scintillation light from alkali halides produced by stopping energetic ions with $2 < Z < 20$ can be described by a single linear function of $E_0^{3/2}/A^{1/2}Z^{2/3}$, where E_0 is the initial energy, and A and Z are the mass number and charge of the incident particle, respectively. Measurements in CsI(Tl) and NaI(Tl) are shown and a brief discussion of the implications of this observation is given.

THE total amount of light produced by heavy charged particles stopping in alkali halide scintillators is known to vary with the type of particle and to show nonlinearity with energy [Fig. 1(a)]. During an investigation of the scintillation properties of CsI(Tl) , we noticed that the total light produced in CsI(Tl) by energetic ions heavier than helium could be described by a linear function of $\epsilon = E_0\beta_0/Z^{2/3} \propto E_0^{3/2}/A^{1/2}Z^{2/3}$, where E_0 is the initial energy of the stopping nuclide, A is its mass number, Z is its nuclear charge, and $c\beta_0$ is its initial velocity. This relation is apparently valid for other alkali halide scintillators as well.

The pulse-height measurements in CsI(Tl) of Quinton *et al.*¹ for nuclides of H^1 , He^4 , C^{12} , N^{14} , and O^{16} , are shown in Fig. 1(a).² The pulse height L is in arbitrary units. Figure 1(b) shows the same data plotted against the

parameter ϵ . The measurements in CsI(Tl) of Newman *et al.*³ and our own data obtained in connection with a fluorescent decay study show similar linear dependence on ϵ with slightly different slopes. The usefulness of this parameter for describing observed pulse heights in CsI(Tl) is emphasized by two further results: First, Newman *et al.*,³ who plotted their pulse-height measurements versus E/A , noted that the curves for N^{14} and B^{11} ions coincided. This is exactly what would be expected from a linear dependence on ϵ . Second, the data of the present authors include measurements of the pulse height from 116 MeV B^{11} ions and 128 MeV C^{12} ions. A linear dependence on ϵ predicts that the boron ions, although of lower total energy, will give a 4% greater pulse height than the carbon. Actual measurement of the relative heights yielded a boron pulse height ($6 \pm 2\%$) higher than the carbon.

The pulse-height measurements of Newman and Steigert⁴ using NaI(Tl) are shown in Fig. 2(a). Points from these curves are plotted against ϵ in Fig. 2(b), and the linear relationship for ions heavier than helium is again demonstrated.

* This work is supported in part through funds provided by the Atomic Energy Commission under contract AT(30-1)-2098.

¹ A. R. Quinton, C. E. Anderson, and W. J. Knox, *Phys. Rev.* **115**, 886 (1959).

² The data of Quinton represent the integrated light output to 1 μsec . Our data on decay times show that for this time interval, only about 70% of the total light was measured for protons, and 80–90% for heavier particles. The measurements for N^{14} with energies less than 25 MeV are due to Halbert [*Phys. Rev.* **107**, 647 (1951)] as cited by Quinton *et al.* in Ref. 1.

³ E. Newman, A. M. Smith, and F. E. Steigert, *Phys. Rev.* **122**, 1520 (1961).

⁴ E. Newman and F. E. Steigert, *Phys. Rev.* **118**, 1575 (1960).